Department of Pharmaceutics[1], China Pharmaceutical University, Nanjing; College of Pharmacy[2], Anhui Medical University, Hefei, China

Synthesis, characterization, drug-loading capacity and safety of novel pH-independent amphiphilic amino acid copolymer micelles

JIHUI TANG[1,2], JING YAO[1], JINGBO SHI[2], QINGPIN XIAO[2], JIANPING ZHOU[1], FEIHU CHEN[2]

Received November 23, 2011, accepted December 28, 2011

Jianping Zhou, Department of Pharmaceutics, China Pharmaceutical University, 24 Tongjiaxiang, Nanjing 210009, China
zhoujpcpu@126.com
Feihu Chen, College of Pharmacy, Anhui Medical University, 81 Meishan Road, Hefei 230032, China
cfhchina@sohu.com

Pharmazie 67: 756–764 (2012) *doi: 10.1691/ph.2012.1152*

A novel block copolymer containing two polymeric components, poly(L-aspartic acid)-b-poly (L-phenylalanine) (PAA-PPA), was synthesized and its potential for the preparation of copolymer micelles with a poorly water-soluble drug was investigated in this study. The chemical structure and physical properties of PAA-PPA were characterized by FTIR, ^{1}H NMR and TG. The degree of polymerization of PAA-PPA was calculated by analyzing the relative area of N-CH signal and C-CH_3 of ^{1}H NMR spectra. The critical micelle concentration (CMC) of the PAA-PPA achieved a minimum of 11.1 mg/L. Studies on the drug-free PAA-PPA solutions showed PAA-PPA aggregation into micellar type in the sub-150 nm size range. Furthermore, the size of the PAA-PPA micelles was found to be pH-independent between the pH range of 4.0 and 8.0, which could be favorable to avoid the limitation of the size change at the specified pH value seeking drug stability. 4-amino-2-trifluoromethyl-phenyl retinate (ATPR) was studied as a poorly water-soluble model drug. The drug-loading and entrapment efficiency of the ATPR-loaded PAA-PPA micelles were 30.9 wt% and 87.9 %, respectively. The high drug-loading and entrapment efficiency were due to the synergistic effect of the micellar encapsulation and the binding interaction between drug and PAA-PPA. The ATPR-loaded PAA-PPA micelles showed a narrow size distribution, low zeta potential, high drug-loading capacity and good stable. The PAA-PPA was safer than Tween-80 and Cremophor EL (CrmEL) as an injectable pharmaceutical adjuvant for ATPR as indicated by the hemolysis and cytotoxicity studies. The novel amphiphilic amino acid copolymer can be considered as a prospective injectable delivery system for ATPR in terms of the pH-independent, greater drug-loading capacity and safety.

1. Introduction

Poly(amino acid)s are well-known as biodegradable and environmentally acceptable materials (Anderson et al. 1974; Makino et al. 1985; Li et al. 1993). Poly(amino acid)s received growing scientific attention in the last four decades. Earlier studies focus on three aspects, i.e. the poly(amino acid)-drug conjugate (Uchino et al. 2005; Schellenberger et al. 2009; Ponta and Bae 2010), poly(amino acid)-other carrier materials conjugate or poly(amino acid)/other carrier materials complex (Romberg 2007; Schlapschy et al. 2007; Romberg et al. 2008; Shu et al. 2009; Wang et al. 2009; Liu et al. 2010; Park et al. 2010; Yang et al. 2010) and amino acid copolymer (Holowka et al. 2007; Sun et al. 2007; Kim et al. 2009). The application of the first two aspects is limited due to the complex preparation technology, great drugs loss, low drug-loading and instability. The amino acid copolymer, especially amphiphilic copolymer, can form micelles, fibers or vesicles through self-assembly. In recent years, the amino acid copolymers attracted a wide spread attention.

The amphiphilic amino acid copolymer-based drug carrier system have some advantages as followed. First, the appropriate ratio of hydrophilic to hydrophobic blocks can form a core-shell type structure by self-aggregation. Second, small particle size promotes escape to tumors and sites of inflammation based on the enhanced permeability and retention (EPR) effect (Matsumura and Maeda 1986). Third, hydrophilic blocks, like poly(ethylene glycol) (PEG), is responsible for a reduced uptake by the reticulo-endothelial system which results in prolonged the micelles circulation times *in vivo* (Gref et al. 1994) while hydrophobic blocks, very close in chemical structure to drug, can improve drug-loading through hydrophobic interactions (Kataoka et al. 1993). Besides, as the preparation of amphiphilic amino acid copolymer-based drug carrier system is achieved by simple mixing of the drug and amphiphilic amino acid copolymer, this method will eliminate the need for a synthetic procedure of attaching the drug to the polymer. Tongjit et al. (1998) showed the aggregate possessed a core–shell-type when the ratio of Ala to Sar blocks was nearly equal to 1. Holowka et al. (2007) reported that the poly(arginine)-b-poly(L-leucine) could entrap the water-soluble species and yield the stable, low-polydispersity vesicles of controllable size down to 50 nm. Sun et al. (2007) synthesized a series of poly(L-lysine)-b-poly(L-phenylalanine), which were used to form 0.55–6 μm vesicles. The poly(g-benzyl L-glutamate)-b-

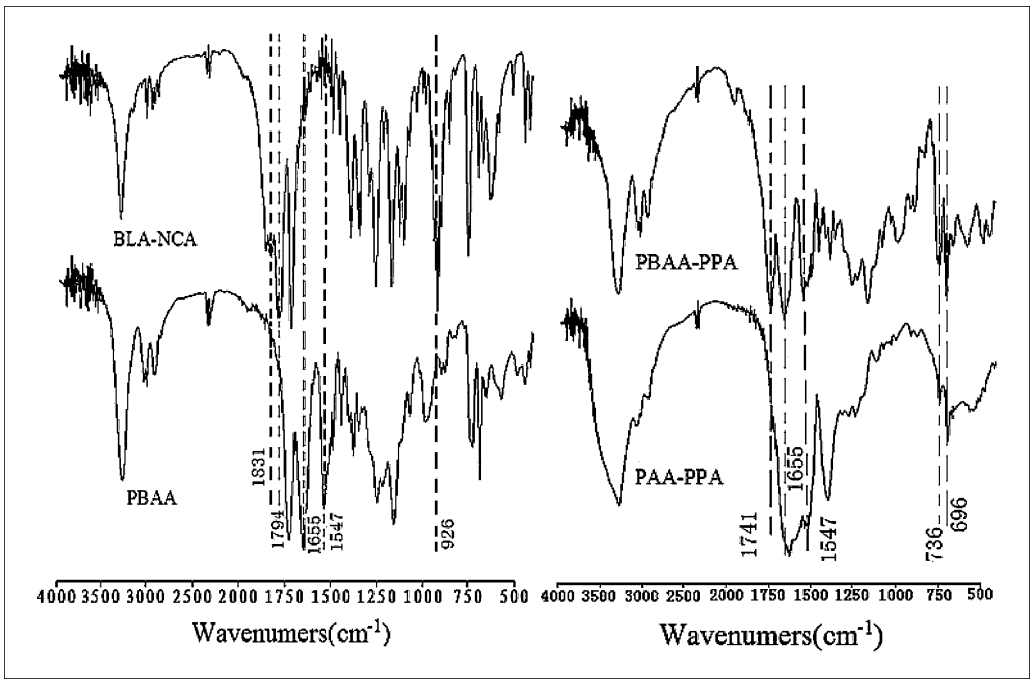

Fig. 1: Infrared spectrum of BLA-NCA and PBAA (left), PBAA-PPA and PAA-PPA (right)

poly(L-phenylalanine) showed the pH-dependent agglomeration due to changes in the PGA ionization state (Kim et al. 2009). However, they offered no any evidence for drug delivery applications. In addition, only the pH-dependent agglomeration may not effectively avoid the change of the particle size at the specified pH value seeking drug stability.

In our study, we synthesized a series of diblock copoly(amino acid)s, poly(L-aspartic acid)-b-poly(L-phenylalanine) (PAA-PPA). With appropriate ratio of hydrophilic PAA block to hydrophobic PPA block, the PAA-PPA can be self-assembled into nano-micelles. The PAA as hydrophilic block can balance the molecular association forces and also to provide steric stabilization of the micelles. The hydrophobic PPA block carries so many phenyl groups are able to form intra- and intermolecular hydrophobic interactions with drugs molecules, in that way, enhancing construct stability towards dissociation,

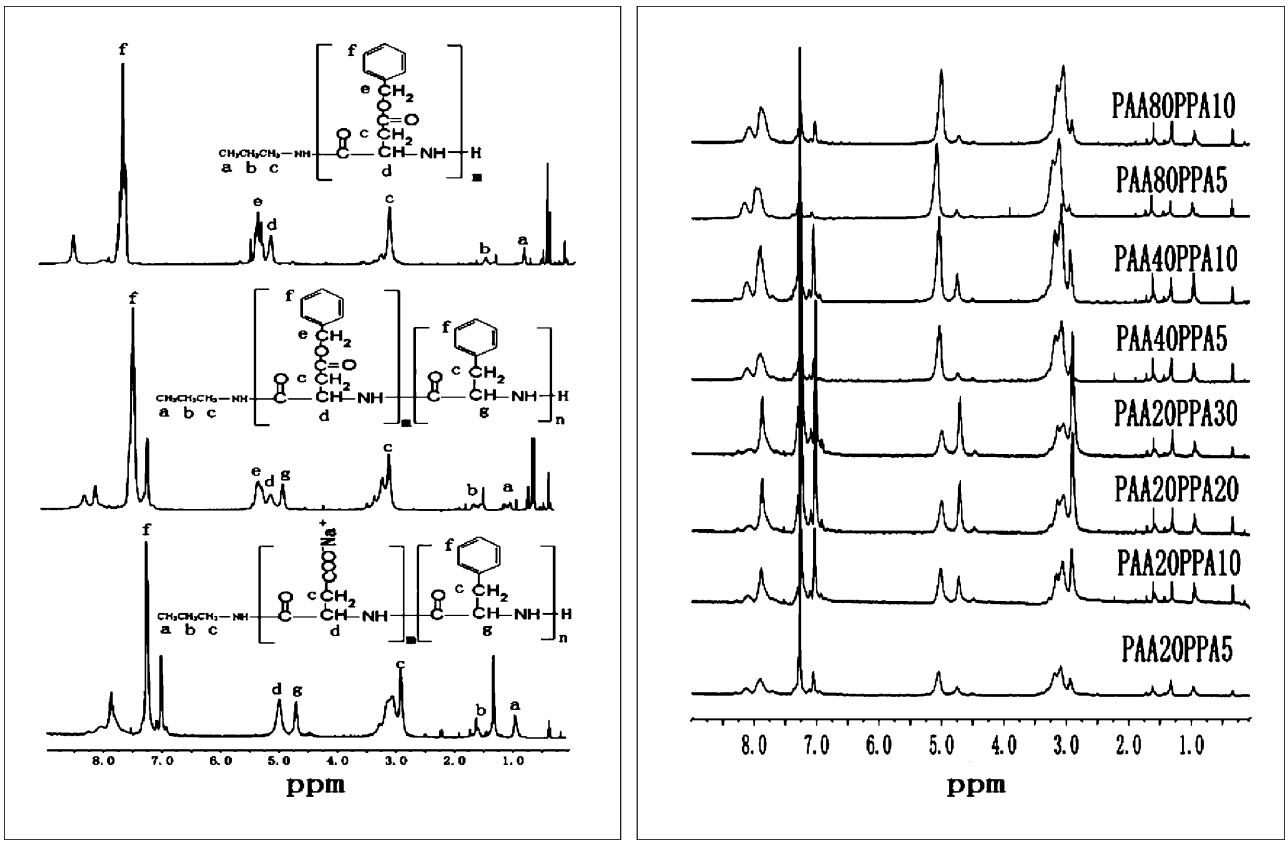

Fig. 2: ^{1}H NMR spectrum of PBAA (left, upper), PBAA-PPA (left, middle), PAA-PPA (left, lower) and a series of PAA-PPA (right)

improve drug-loading and consequently possibly reducing the drug-release rate. Besides, interestedly, the pH value of the disperse medium did not affect on the size of the PAA-PPA-based micelles, which was favorable to keep the drug stable.

The 4-amino-2-trifluoromethyl-phenyl retinate (ATPR) was screened from a series of all-trans retinoic acid (ATRA) and ATRA derivatives by our team. The anti-tumor activities of ATPR against NB4 and K562 cell lines were evaluated *in vitro* by MTT assays. After treatment with ATPR, most NB4 and K562 cells showed to be increased in the G1 phase and reduced in the S phases. The results indicated that ATPR exhibited superior inducing differentiation activity to that of ATRA (Ruan et al. 2009; Shen et al. 2009). However, ATPR will be degraded in an aqueous medium under acidic, alkaline and light catalysis. Furthermore, the poorly water-soluble of ATPR (0.64 μg/mL), made it difficult to prepare a commercial formulation. Because of the inherent problems associated with ATPR, using a suitable method to improve the solubility and stability of ATPR is very important. It may not be a good idea to prepare the prodrug of ATPR for improving its solubility due to degradation of the ATPR during the synthesis process. On the other hand, although low molecular weight surfactants such as Tween and CrmEL can also improve the solubility of ATPR, they may generate significant side effects after iv administration. Based on the advantages of the polymer micelles including high drug loading, stability, drug protection and easy production, it is appropriate as the carrier of ATPR to improve its solubility and stability.

In this study, the synthesis of a series of two polymeric components, poly(L-aspartic acid)-b-poly(L-phenylalanine), was presented. The chemical structure and physical properties of PAA-PPA were characterized by FTIR, ^{1}H NMR and TG. The critical micelle concentrations (CMCs) of PAA-PPA were determined by pyrene fluorescence probe spectrometry. The formation of micelles from PAA-PPA and physicochemical characterisation in terms of the size and morphology of the micelles were also reported. Then we took ATPR as a poorly water-soluble model drug to study the physical properties, characteristics and safety of ATPR-loaded PAA-PPA micelles and its drug-loading capacity for ATPR, which would helpful to find applications as drug delivery systems.

2. Investigations, results, and discussion

2.1. Evidence of living polymerization and the thermally stable of PAA-PPA

The PAA-PPA was synthesized by ring-opening polymerization of NCA (Deming 2000; Aliferis et al. 2004). The PAA-PPA was analyzed by infrared spectrum and ^{1}H NMR spectrum. As shown in Fig. 1 (left), the characteristic absorption peak of BLA-NCA 926 cm^{-1}, 1831 cm^{-1}, 1794 cm^{-1} disappeared when added n-propylamine to BLA-NCA solution and stirred for 1 day. The absorption peak of 1655 cm^{-1} (-NH-(CO)- Carbonyl stretching vibration), 1547 cm^{-1} (amide II band N-H formation vibration) appeared in the FTIR spectra of PBAA. This indicates that BLA-NCA consumed completely and created PBAA. Compared with the spectrum of PAA-PPA (Fig. 1 (right)), the benzyl ester carbonyl stretching vibration signal (1741 cm^{-1}) of PBAA almost disappeared and benzene ring out-of-plane bending vibration signal (736 cm^{-1}, 696 cm^{-1}) declined after the removing protection group reaction. The infrared signal on 1655 cm^{-1} (-NH-(CO)- Carbonyl stretching vibration), 1547 cm^{-1} (amide II band N-H formation vibration) unchanged. This showed that a successful debenzylation was achieved.

Fig. 2 (left) shows the ^{1}H NMR spectrum of PBAA, PBAA-PPA, PAA-PPA. The -CH_2- proton (5.13 ppm) of benzyl ester disappeared in the ^{1}H NMR spectrum of the product. This confirmed that successful debenzylation was accomplished. The molecular weight was calculated from the integrated value of the ^{1}H NMR data. The integrated value ratio of -CH- proton signal (4.98 ppm) of PAA to -CH_3 proton signal (0.91 ppm) of n-propylamine was used for calculating the degree of polymerization of PAA, while the -CH- proton signal (4.69 ppm) of PPA and -CH_3 proton signal of n-propylamine were used for the degree of polymerization of PPA. For optimization an appropriate ratio, we synthesized a series of PAA-PPA (see Fig. 2 (right)): PAA20PPA5, PAA20PPA10, PAA20PPA20, PAA20PPA30, PAA40PPA5, PAA40PPA10, PAA80PPA5 and PAA80PPA10, the digital represents the feeding molar ratio of NCA to the initiator.

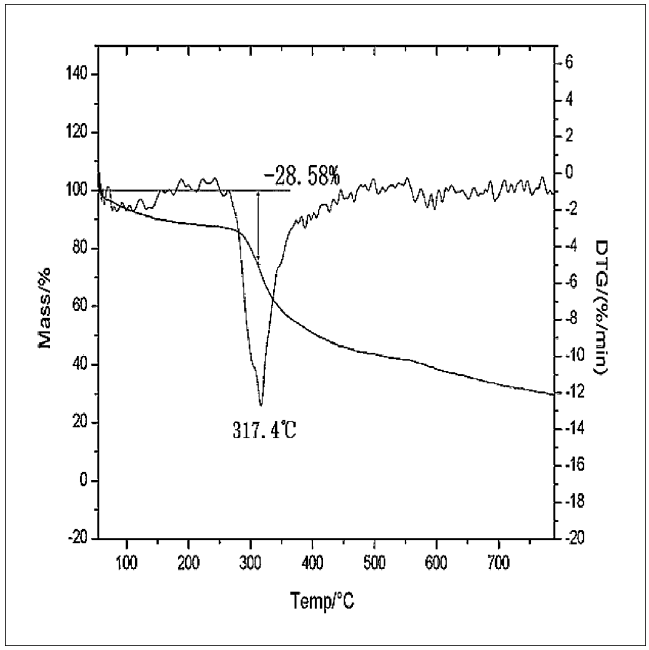

Fig. 3: TG thermogram of PAA20PPA20

TG thermogram of PAA20PPA20 is shown in Fig. 3. PAA20PPA20 lost 28.58 % of its weight at the peak of DTG (317.4 °C). This indicated that PAA-PPA was thermally stable.

2.2. Characterisation of blank PAA-PPA micelles

The size of the blank PAA-PPA micelles (Table 1) measured by a DLS analyzer was smaller than 150 nm with the polydispersity index (PDI) in the range from 0.144 to 0.480, and Fig. 4 showed that spherical aggregates were formed in water. Contrary to previous results with the poly(L-lysine)-block-poly(L-phenylalanine) (Sun et al. 2007) that formed large vesicles (on micrometer scale) spontaneously, the poly(L-aspartic acid) introduced to the structure of PAA-PPA copolymer resulted in the formation of a micellar system (on nanometer scale, see Fig. 4). Amphiphilic amino acid copolymer can form a variety of structures, including micelles, fibers, and vesicles, via intermolecular or intramolecular hydrogen bonding, hydrophobic interactions and π-π stacking (Kim et al. 2009). The primary driving force responsible for the aggregation behavior is the minimization of the interfacial energy governed by the balance between the hydrophilic block and the hydrophobic block of the amphiphilic amino acid copolymer (Barrio et al. 2010). Compared with the hydrophilic block of the poly(L-lysine)-block-poly(L-phenylalanine), the hydrophilic block of the PAA-PPA is poly(L-aspartic acid) sodium salt, the more hydrophilic of the poly(L-aspartic acid) sodium salt than poly(L-

Table 1: Molar ratio, molecular weights, average size, polydispersity, zeta potential and CMC of a series of PAA-PPA

	Calculated molar ratio	Molecular weights (Da)	Zeta potential	Size (nm) (PDI)	CMC (mg/L)
PAA20PPA5	20.3:3.5	3355	−55.2	120.5 ± 5.4 (0.218)	34.0
PAA20PPA10	17.8:8.9	3806	−56.2	105.6 ± 9.7 (0.144)	20.6
PAA20PPA20	15.4:15.3	4418	−54.8	121.6 ± 3.4 (0.144)	13.1
PAA20PPA30	15.6:22.9	5563	−55.7	116.6 ± 12.0 (0.144)	11.1
PAA40PPA5	25.2:2.0	3805	−40.1	125.0 ± 107 (0.417)	94.8
PAA40PPA10	29.8:6.5	5097	−46.2	123.8 ± 10.5 (0.195)	69.2
PAA80PPA5	45.9:2.5	6715	−50.4	138.3 ± 9.5 (0.381)	246.5
PAA80PPA10	49.7:4.9	7588	−48.6	128.5 ± 7.4 (0.480)	105.7

The size and zeta potential values represent the mean ± S.D. from three independent experiments

lysine) can stabilize a larger surface area and produced a micellar system with smaller size. This is the same as the poly(L-glutamic acid) sodium salt composed of the hydrophilic block of the poly(L-glutamic acid)-block-poly-(L-phenylalanine) (Kim et al. 2009).

The size of micelles and the parameter of CMC are two critical factors that should be taken into account. The size of the micelle smaller than 200 nm can promote escape to tumors and sites of inflammation based on the enhanced permeability and retention (EPR) effect. The parameter of CMC is a very critical indicator of micellization ability and micelle stability: the lower the CMC value means the more stable the micelle (Li and Bae 2006). As we can see from the Table 1, increasing the PPA block chain length will decrease the CMC but the micelle size changed regardless of the chain length, this may be explained by an increased repulsion when the chain gains more charges (Li and Bae 2006), such as PEG-b-PLL/plasmid DNA complex micelles and PEG-b-P(Asp)/PLL (Harada and Kataoka 1997; Katayose and Kataoka 1998). The zeta potentials is another indicator of micelle stability. As we can see from the Table 1, all of the zeta potentials were less than −40 mV, which indicates the aqueous stability for the PAA-PPA micelles (Si and Samulski 2008).

Many studies have reported the use poly(amino acid)s as pH sensitive drug delivery systems, such as poly(L-glutamic acid)-b-poly-(L-phenylalanine) (Kim et al. 2009) and PEG-b-Poly(aspartic acid-stat-phenylalanine) (Prompruk et al. 2005). Although this character is beneficial for controlling drug release, it is not always popular. We know the pH values changing more or less during the preparation, transportation and storage. Sometimes, it may be favorable in terms of pH-independence to avoid the limitation of the size change at a specified pH value seeking drug stability. The size of PAA20PPA20-based nanoparticles at different pH values were in the range from 122 to 134 nm (Fig. 5). There were no significant changes in size at different pH values compared with that of poly(L-glutamic acid)-b-poly-(L-phenylalanine) (Kim et al. 2009), poly(L-lysine)-block-poly(L-phenylalanine) (Sun et al. 2007), Poly(L-glutamic acid)-block-Poly(lactic-co-glycolic acid) copolymers (Yang et al. 2010) and PEG-b-Poly(aspartic acid-stat-phenylalanine) (Prompruk et al. 2005).

The pH sensitivity of the poly(amino acid)s can be elucidated by the poly(amino acid)s ionization. For example, poly(aspartic acid) would be 95.2 % ionized at pH 5.3 (if the pKa value is taken as 4.0). At pH 2, (poly(aspartic acid) would be only 0.99% ionized. The reduced ionization of the carboxylic acid groups of the PEG-P(asp-phe) polymer would be expected to result in reduced repulsive forces, which consequently led to a decreasing size (Prompruk et al. 2005). As another reason, the ionized carboxylic groups of PEG-P(asp-phe) located inside the core attracted the solvent into the cores of the micelles, resulting in the increase of inner aqueous phase and the expansion of micelles size (Yang et al. 2010). As for the PAA-PPA, it would be ionized like that of PEG-P(asp-phe), but the poly(aspartic acid) block

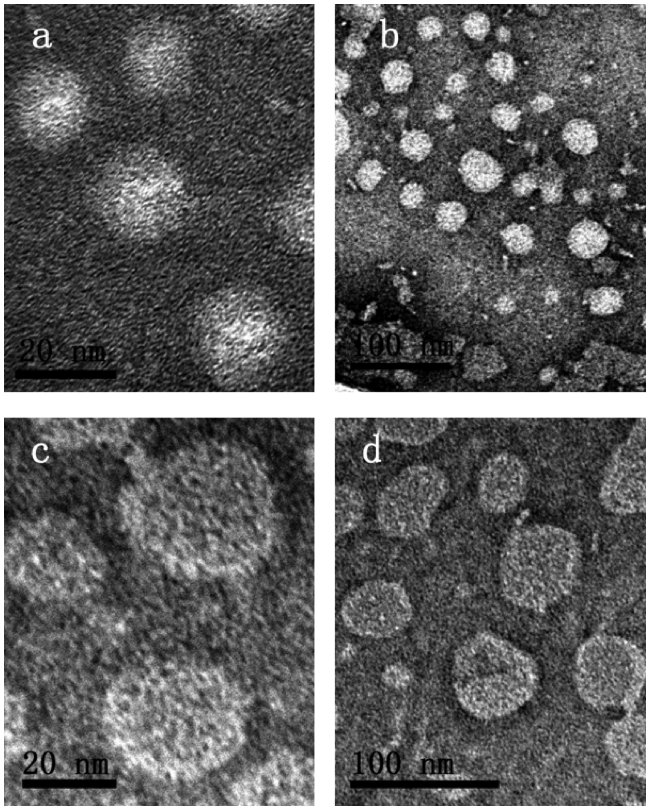

Fig. 4: Transmission electron microscopic (TEM) images of PAA20PPA20 micelles without ((a) and (b)) and with ((c) and (d)) ATPR

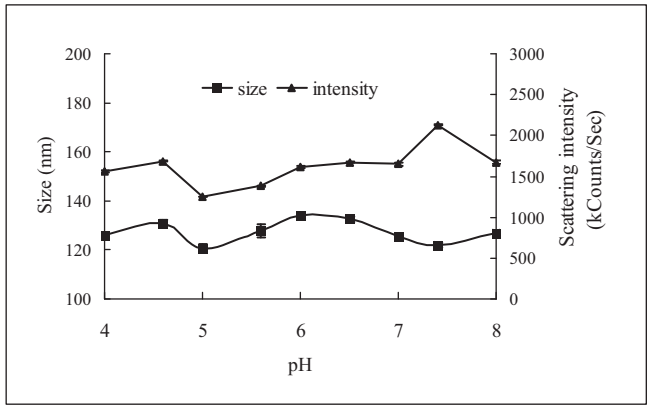

Fig. 5: Effect of pH on the size and scattering intensity of the blank PAA20PPA20 micelles

of PAA-PPA in the shell of the PAA-PPA micelles, the distance between molecules of the poly(aspartic) acid block of PAA-PPA might big enough to slacking down the charge repulsive forces. Moreover, the outer poly(aspartic acid) block would not attract the solvent into the cores of the micelles. Compared with poly(L-glutamic acid)-b-poly-(L-phenylalanine), which kept the micelles size uniformly above pH 6.0, the PAA-PPA kept the micelles size uniformly above pH 4.0, this may be L-aspartic acid with lower isoelectric point can be ionised insignificantly (Kim et al. 2009).

Light scattering, indicative of molecular assembly (Prompruk et al. 2005), was observed for the aqueous buffer solutions of PAA20PPA20 at different pH values. The light-scattering values of PAA20PPA20-based micelles at different pH values remained almost unchanged (Fig. 5). Since there was no distinct change in the light- cattering curve profile, this implied that the molecular assembly of PAA-PPA remained unaffected by the pH values in the range from 4.0 to 8.0.

Considering the zeta potentials (−30 mv– −40 mv, data not shown), PDI ($\leq$0.2, data not shown), size and scattering inensity of the PAA-PPA micelles at different pH values, it was considered that the PAA-PPA micelles exhibited pH-independent properties.

2.3. Incorporation of ATPR into the PAA-PPA micelles and characterization of ATPR-loaded PAA-PPA micelles

ATPR-loaded PAA-PPA micelles were prepared by dialysis method through physically incorporated within the hydrophobic cores. A clear and homogenous ATPR-loaded PAA-PPA micelles solution was obtained. Drug-loading capacity of the PAA-PPA is listed in Table 2. The amount of free ATPR was not taken into account when calculating the drug-loading and entrapment efficiency of ATPR-loaded PAA-PPA micelles because of the few ATPR dissolved in water. The drug-loading and entrapment efficiency of the ATPR-loaded PAA-PPA micelle achieved a maximum of 30.9 wt% and 87.9 %, respectively. The drug-loading capacity enhanced with the increasing of the hydrophobic chain (except for PAA20PPA30, which was lost in the filtering process because of the low solubility of PAA20PPA30 in water). This result could be explained by the fact that the longer the PPA chain, the stronger binding affinity between ATPR and the hydrophobic chain. This is the same as doxorubicin-loaded poly(ethylene glycol)–poly(b-benzyl-L-aspartate) copolymer micelles (Kataoka et al. 2000) and PTX-loaded octyl modified serum albumin micelles (Gong et al. 2009). The longer PBLA chain length in the poly(ethylene glycol)–poly(b-benzyl-L-aspartate) means improving the loading capacity of DOX in the micelles. The drug-loading capacity enhanced with the increasing of the degree of substitution of octyl group in the octyl modified serum albumin micelles system.

From Table 2, we can see the sizes of ATPR-loaded micelles were below 160 nm with narrow size distribution, which will result in long circulation times and increasing accumulation in tumor tissue by EPR effect (Li and Bae 2006). Zeta potentials was less than −55 mv after drug-loading, which indicated the aqueous stability for the ATPR-loaded PAA-PPA micelles (Si and Samulski 2008).

The stability of ATPR-loaded PAA-PPA micelles is also shown in Table 2. All preparations were stable for more than 8 days, 1 day and 1 day at 4 °C, 25 °C and 37 °C, respectively. However, ATPR dissolved in water was stable only 3 days at 4 °C, no more than 1 day at 25 °C and 37 °C, respectively (data not shown). The results were consistent with previous studies of the PTX-loaded octyl modified serum albumin micelles (Gong et al. 2009). This

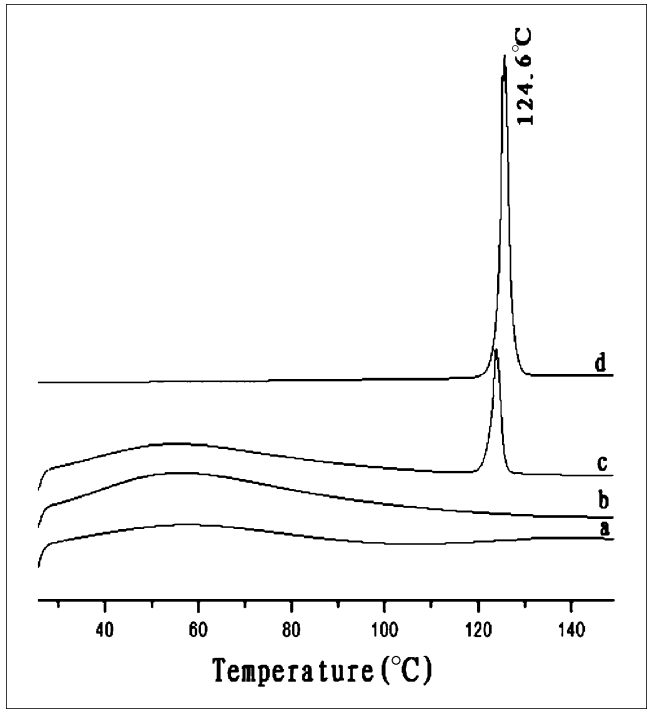

Fig. 6: DSC thermograms of PAA20PPA20 (a), ATPR-loaded PAA20PPA20 micelles (b), physical mixture of ATPR and PAA20PPA20 (c) and ATPR (d)

may be explained by the fact of the stronger hydrophobic interaction between ATPR and the hydrophobic segment of PAA-PPA. Moreover, the size had no significant changes (data not shown) during the experiment. These results indicated that the relative instability of ATPR-loaded PAA-PPA micelles was not induced by the aggregation of PAA-PPA micelles but some other reasons, such as drug releasing, light and heat.

DSC diagrams of PAA20PPA20, ATPR, physical mixture of PAA20PPA20 and ATPR and ATPR-loaded PAA20PPA20 micelles are shown in Fig. 6. We can see a ATPR melting endothermic peak (124.6 °C), but there were no distinct peak in the DSC diagrams of PAA20PPA20 and ATPR-loaded PAA20PPA20 micelles. These demonstrated that ATPR existed in the PAA-PPA micelles with the state of solid dispersion or amorphism.

2.4. In vitro drug release of ATPR from ATPR-loaded PAA-PPA micelles

Figure 7 illustrates the release profiles of ATPR from ATPR-loaded PAA-PPA micelles. All of the ATPR-loaded PAA-PPA micelles displayed a rapid release within 1 h and followed by slow and sustained release for a prolonged period of time. The previously reported drug-loaded of PEG-block-poly(aspartic acid-stat-phenylalanine) copolymer micelles (Yang et al. 2010) and poly(ethylene glycol)–poly(b-benzyl-L-aspartate) copolymer micelles (Kataoka et al. 2000) were also displayed a rapid release. The reason for rapid release of the drug within 1 h during the release study is not clear. It may be the higher temperature (37 °C) during the release experiment and manipulations with the sample to set up the release experiment. The sustained release of ATPR from the ATPR-loaded PAA-PPA micelles due to the introduction of the phenylalanine group in the structure of PAA-PPA copolymer (Yang et al. 2010).

2.5. Hemolysis test

Amphiphilic materials such as phospholipids, Tween-80, Poloxamer188 and CrmEL, can solubilize or be inserted into cell

Table 2: Average size, polydispersity, zeta potential, drug-loading, entrapment efficiency and stability of a series of ATPR-loaded PAA-PPA micelles

	Size(nm) (PDI)	Zeta potential	DL (wt%)	EE (%)	Stability (d)		
					4 °C	25 °C	37 °C
PAA20PPA5	283.6 ± 15.3 (0.156)	−70.8	27.3	74.1	10	1	1
PAA20PPA10	238.1 ± 21.9 (0.269)	−69.7	28.0	76.7	13	1	1
PAA20PPA20	145.3 ± 13.9 (0.148)	−65.3	30.9	87.9	> 14	2	1
PAA20PPA30	126.2 ± 10.9 (0.401)	−70.4	20.1	49.6	10	1	1
PAA40PPA5	152.6 ± 12.7 (0.242)	−56.0	27.6	74.4	8	1	1
PAA40PPA10	148.7 ± 10.6 (0.242)	−61.7	29.5	81.0	10	1	1
PAA80PPA5	158.3 ± 11.0 (0.298)	−57.8	29.2	80.3	10	1	1
PAA80PPA10	149.0 ± 7.8 (0.235)	−59.6	29.3	80.8	10	1	1

The size, zeta potential, DL and EE values represent the mean ± S.D. from three independent experiments

membranes, which leads to hemolysis of red blood cells (RBCs). Hemolysis test is necessary for new amphiphilic compounds. The hemolysis of PAA20PPA20 was compared with CrmEL and Tween-80. Figure 8, a and b shows that the hemolysis of Tween-80 sharply increased from 15.6 % to 29.5 % at concentrations between 0.8 mg/mL and 4 mg/mL, while the hemolysis of PAA20PPA20 was negligible and similar to that of CrmEL. Meanwhile, ATPR-loaded PAA20PPA20 micelles demonstrated a hemolytic activity of 1.9 % at a concentration of 0.2 mg/mL, a little lower than that 3.6 % of ATPR solution in CrmEL at the same concentration. These indicated that the PAA-PPA micelles would be nontoxic towards erythrocytes after intravenous injection.

2.6. In vitro cytotoxicity studies

The cytotoxicity of ATPR-loaded PAA20PPA20 micelles and ATPR solution in CrmEL was evaluated with NB4 cells by MTT cell proliferation assay. The experiment was designed at the ATPR concentration of drug-loading formulation between 0.00046 μg/mL and 4.6 μg/mL and the corresponding amphiphilic materials concentration between 0.00092 μg/mL and 9.2 μg/mL. As shown in Fig. 8c the cell viabilities of PAA20PPA20 were approximately 100 % during the detected concentrations while those CrmEL were 87.7 % and 69.1 % at the concentration of 0.092 μg/mL and 9.2 μg/mL, respectively. Therefore, it can be expected that PAA-PPA micelles were far less toxic than Cremophor EL vehicle. Figure 8d indicates the cell viabilities of ATPR-loaded PAA20PPA20 micelles were similar to that of ATPR CrmEL solution, which indicated that ATPR remained biologically active after being incorporated into PAA20PPA20 micelles. ATPR CrmEL solution showed strong cytotoxicity at 0.046 μg/mL, 0.46 μg/mL and 4.6 μg/mL, which may be attributed partially to the use of Cremophor EL vehicle. In contrast, the cytotoxicity of ATPR-loaded PAA20PPA20 micelles was more likely induced by ATPR itself (Huo et al. 2010). In conclusion, PAA-PPA was a safer injectable pharmaceutic adjuvant and ATPR-loaded PAA-PPA preparation cannot affect the antitumor activity.

2.7. Conclusions

The synthesis of a novel block copolymer containing two polymeric components, L-aspartic acid and L-phenylalanine and its potential for the preparation of copolymer micelles with a poorly water-soluble drug were investigated in this study. The CMC of PAA-PPA achieved a minimum of 11.1 mg/L. Initial studies on the drug-free PAA-PPA solutions indicated PAA-PPA aggregation into micellar type in the sub-150 nm size range. Furthermore, the size of the PAA-PPA micelles was found to be pH-independent between the pH values range of 4.0 and 8.0, which could be favorable to avoid the limitation of the size change at the specified pH value seeking drug stability.

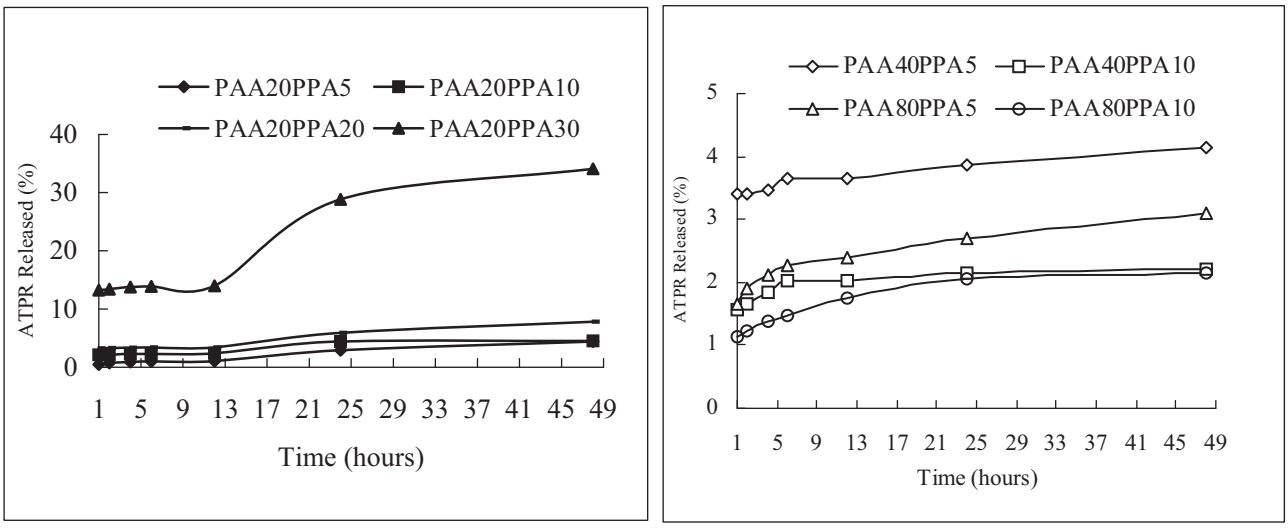

(a) (b)

Fig. 7: *In vitro* drug-release of ATPR-loaded PAA20PPA5, PAA20PPA10, PAA20PPA20, PAA20PPA30 (a), PAA40PPA5, PAA40PPA10, PAA80PPA5, and PAA80PPA10 (b) micelles

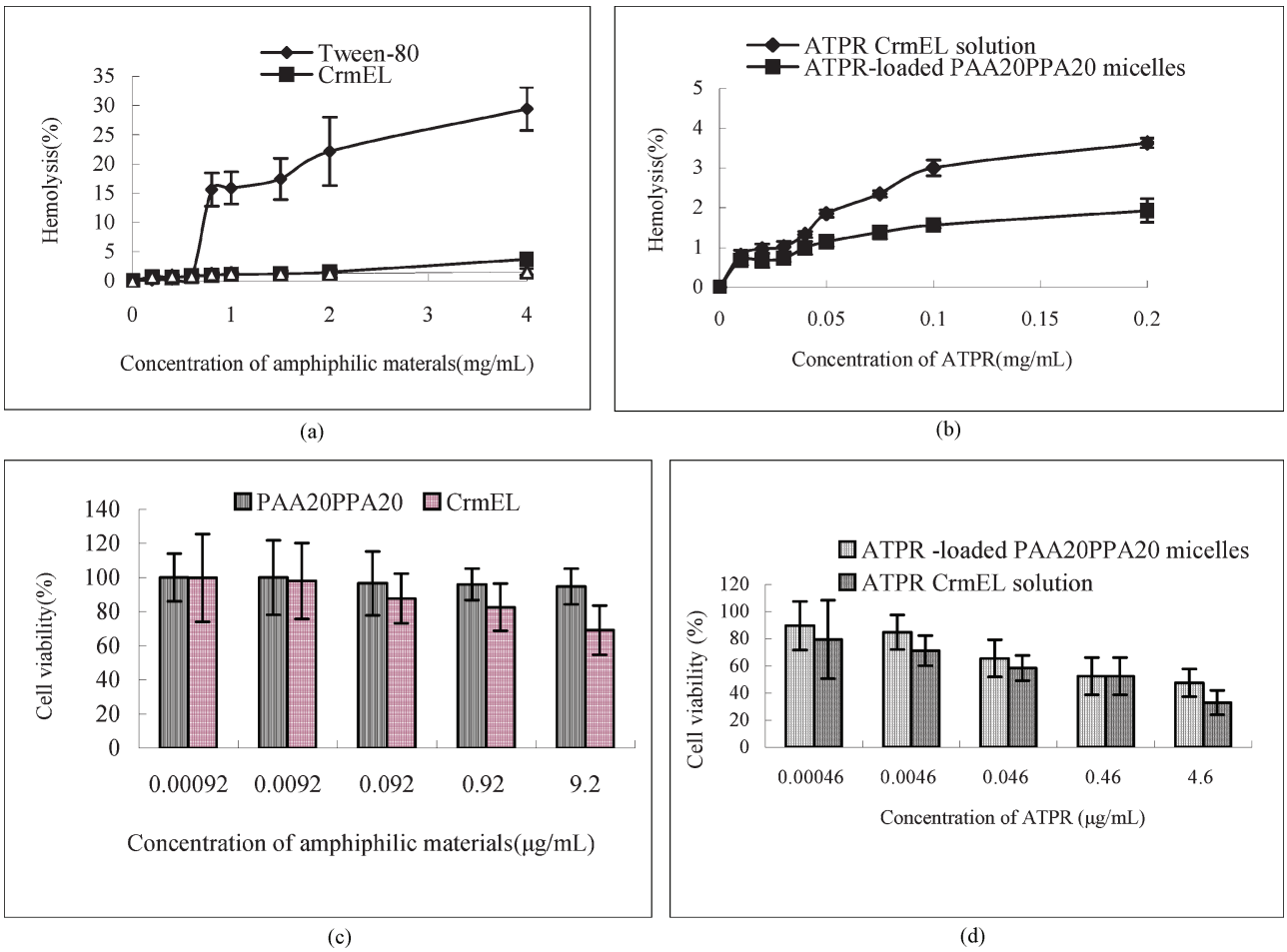

Fig. 8: Hemolysis test (a and b) and cytotoxicity studies (c and d) results of amphiphilic materals Tween-80, CrmEL, PAA20PPA20, and ATPR CrmEL solution and ATPR-loaded PAA20PPA20 micelles. Each datum represents the mean ± S.D. from three independent experiments (hemolysis test) and six independent experiments (cytotoxicity studies)

ATPR was studied as a model drug. The drug-loading and entrapment efficiency of the PAA-PPA micelle were 30.9 wt% and 87.9 %, respectively. The high drug-loading and entrapment efficiency were due to the synergistic effect of the micellar encapsulation and the binding interaction between drug and PAA-PPA. The ATPR-loaded PAA-PPA micelles showed a narrow size distribution, a low zeta potential, a high drug-loading capacity and good stable. The PAA-PPA was safer than Tween-80 and CrmEL as an injectable pharmaceutical adjuvant for ATPR as indicated by the hemolysis and cytotoxicity studies. The novel amphiphilic amino acid copolymer can be considered as a prospective injectable delivery system for ATPR in terms of the pH-independent, greater drug-loading capacity and safety.

Considering the size, stability and drug loading of the PAA-PPA micelles, it was considered that the chain length of PAA20PPA20 may be most appropriate for ATPR, and the pharmacokinetics, biodistribution and efficacy of ATPR-loaded PAA-PPA micelles are being carried out.

3. Experimental

3.1. Materials

L-Aspartic acid β-benzyl ester and L-phenylalanine were purchased from Shanghai Hanhong Chemical Co., Ltd; Tetrahydrofuran (THF), anhydrous ether, *n*-hexane, *N*,*N*-dimethylformamide (DMF), *n*-propylamine and triphosgene were purchased from Sinopharm Chemical Reagent Co., Ltd; DMF, THF, anhydrous ether, and *n*-propylamine were dried with 4 Å molecular sieve for more than three days before used.

3.2. Synthesis of poly(L-aspartic acid)-b-poly-(L-phenylalanine)

Poly(L-aspartic acid)-*b*-poly(L-phenylalanine) (PAA-PPA) was prepared from *N*-carboxy a-amino acid anhydride (NCA) as reported previously (Daly and Poche 1988). L-Aspartic acid β-benzyl ester NCA (BLA-NCA) was polymerized by using *n*-propylamine as the initiator in DMF for one day at room temperature. After complete consumption of BLA-NCA, an excess amount of diethyl ether was added to the solution to acquire poly(L-aspartic acid β-benzyl ester) (PBAA). A DMF solution of L-phenylalanine NCA was added to the DMF solution of PBAA and stirred for one day at room temperature. The mixture was precipitated with an excess amount of diethyl ether to acquire poly(L-aspartic acid β-benzyl ester)-*b*-poly(L-phenylalanine) (PBAA-PPA). To synthesize PAA-PPA, the PBAA-PPA was stirred in 1 M NaOH aqueous solution and dialyzed through a dialysis membrane bag (Spectra/Por MWCO 3500) in deionized water for one day. After two days of freeze drying, PAA-PPA was collected. The degree of polymerization was controlled by the molar ratio of the NCA and the initiator. Analysis was done by measuring the relative area of C-CH_3 signal and N-CH signal of ^{1}H NMR spectra.

3.3. Characterization of PAA-PPA

PBAA, PBAA-PPA, and PAA-PPA were examined with infrared spectroscopy (Shimadzu IR Rrestige-21, Japan). The poly(amino acid)s were dissolved in a 1:1 ratio of TFA and $CDCL_3$ and characterized by ^{1}H NMR spectroscopy (Bruker AVANCE III 400, Germany). The degree of polymerization was computed by measuring the relative area of C-CH_3 signal and N-CH signal of ^{1}H NMR spectra. A NETZSCH STA449 F3 was used to record the TG thermograms. The temperature range was 55–800 °C and the heating rate was 20 °C /min.

3.4. Preparation and characterization of blank PAA-PPA micelles and determination of critical micelle concentration (CMC)

Blank PAA-PPA micelles were prepared by dissolving the PAA-PPA into deionized water at a concentration of 0.5 mg/mL. Zetasizer Nano ZS90

(Malvern, UK) was used to measure the size and zeta potential of the blank PAA-PPA micelles. The morphology of the blank PAA-PPA micelles was observed using a transmission electron microscope (Jeol JEM-2100, Japan) operated at an acceleration voltage of 200 kV, after the solution negatively stained with 2 % (w/v) phosphotungstic acid.The influence of pH values on the size of PAA-PPA micelles was studied at pH 4.0, 4.6, 5.0 and 5.6 (0.01 M acetate buffer), pH 6.0, 6.5, 7.0, 7.4 and 8.0 (0.01 M phosphate buffer).
CMC of PAA-PPA was determined by the fluorescence spectroscopy, using pyrene as the probe. Briefly, 1 mL of 6.0×10^{-6} M pyrene solution in acetone was added into a series of 10 mL volumetric flask and evaporated at room temperature. About 10 mL of different concentrations of PAA-PPA solutions (2×10^{-4} to 5 mg/mL) were placed into the volumetric flasks and sonicated for 30 min. Resulting solutions were heated at 50 °C for 1 h, and then left to be cool at room temperature for overnight. Fluorescent spectrophotometer was used to detect the pyrene excitation spectra at a wavelength of 390 nm. The excitation and emission slit-widths were 3 and 5 nm, respectively (Wilhelm et al. 1991; Gong et al. 2009).

3.5. Preparation and characterization of ATPR-loaded PAA-PPA micelles

ATPR-loaded PAA-PPA micelles were prepared by the dialysis method (Gong et al. 2009). The PAA-PPA solution was prepared by dissolving 60 mg of PAA-PPA in 10 mL of water and stirring for 20 min at room temperature. While stirring of the PAA-PPA solution, a solution of ATPR (30 mg) in 3 mL of DMSO was added dropwise then sonicated for 30 min (JY 92-IID ultrasonic processor, China) under cooling condition. The PAA-PPA solution was dialyzed through a dialysis membrane bag (MWCO 3500) in distilled water for 12 h at 4 °C. The retention of the dialysis was centrifuged at 3000 rpm for 10 min and filtered through a 0.8 μm pore-sized microporous membrane and finally the filtrate was subjected for lypholization. Size, zeta potential and morphology of the ATPR-loaded PAA-PPA micelles were measured as described in section 3.4. Differential scanning calorimeter (DSC) thermograms were collected with a Q2000 DSC equipment. The temperature range and heating rate were 25–150 °C and 10 °C/min, respectively.
The content of ATPR within the ATPR-loaded PAA20PPA20 micelles and the size were tested for studying the stability of ATPR-loaded PAA-PPA micelles at 4, 25 and 37 °C. The blank PAA20PPA20 micelles were measured for comparison.

3.6. Determination of drug-loading and entrapment efficiency

The drug-loading (DL) and entrapment efficiency (EE) were defined as:

$$\text{Drug loading}\,(\%) = \frac{\text{weight of ATPR in micelles}}{\text{weight of TPR in micelles} + \text{weight of carrier fed initially}} \times 100$$

$$\text{Entrapment efficiency}\,(\%) = \frac{\text{weight of ATPR in micelles}}{\text{weight of ATPR fed initially}} \times 100$$

The concentration of ATPR was determined by reverse-phase HPLC (Shimadzu LC-20AT system, Japan) equipped with a Hypersil ODS2 column (5 μm particle size, 250 mm × 4.6 mm). The mobile phase consisted of methanol and water (92:8, v/v) with a flow rate of 1.0 mL/min and the detection wavelength was 367 nm (Shimadzu SPD-20AV UV detector, Japan). The injection volume was 20 μL. To prepare the test sample, the lyophilized powder was dissolved in double distilled water and diluted with methanol (to destroy PAA-PPA micelles and dissolve ATPR). The calibration curve and correlation coefficient were A = 135.9 C+141.0 and 0.9999, the A (mAUs) means integrated area, the C (40–2000 ng/mL) stands for the concentration of ATPR.

3.7. In vitro drug release of ATPR from the ATPR-loaded PAA-PPA micelles

The *in vitro* release of ATPR from the ATPR-loaded PAA-PPA micelles was determined using the dialysis method. The lyophilized power of ATPR-loaded PAA-PPA micelles was dissolved in 0.9 % NaCl solution at a concentration of 0.5 mg/mL. The solution of ATPR-loaded PAA-PPA micelles (1 mL) was added into a dialysis bag (MWCO3500) and dialysed against phosphate buffer solution (pH 7.4, 10 mM, 50 mL, 37 °C) containing 0.2 % Tween 80 so as to achieve sink conditions. The dialysis solution was placed in a water bath and shaken at 100 rpm 37 °C (SHA-C, China). The release medium (20 μL) was analyzed as described in section 3.6 at given time intervals (1, 2, 4, 6,12, 24, 48 h).

3.8. Hemolysis test (Gong et al. 2009)

Rabbit blood was freshly drawn from heart. The blood was stirred promptly to remove the fibrinogen. Sodium chloride solution 0.9 % was used to wash the blood samples by centrifugation at 3000 rpm for 5 min. The supernatant was collected and the procedure was repeated for three times. Red blood cells (RBCs) 2 % v/v suspension was prepared using 0.9 % NaCl solution. The lyophilized power of PAA20PPA20 and ATPR-loaded PAA20PPA20 micelles were dissolved in 0.9 % NaCl at a concentration of 10 and 0.5 mg/mL, respectively. Samples for hemolysis test were prepared by adding 2.5 mL of the prepared RBCs solution to different volumes (0.1–2 mL) of Tween-80, CrmEL and ATPR solution in CrmEL. Sodium chloride 0.9 % solution was added to adjust the volume of the samples up to 5 mL. Positive control (100 % hemolysis) and negative control (0 % hemolysis) samples were prepared by adding to 2.5 mL of 2 % RBCs suspension, 0.9 % NaCl and water up to 5 mL, respectively. The samples were incubated at 37 °C for 30 min, then centrifuged at 3000 rpm for 10 min to remove the intact RBCs. Supernatant was withdrawn and analyzed by spectrophotometric method at 540 nm. The degree of hemolysis was calculated according to the following equation:

$$\text{Hemolysis}\,(\%) = \frac{A_{\text{sample}} - A_{0\%}}{A_{100\%} - A_{0\%}} \times 100$$

3.9. In vitro cytotoxicity studies (Gong et al. 2009)

The NB4 cells were seeded at 5×10^3 cells in each well of 96-well plates, respectively, then incubated at 37 °C for 4 h. The ATPR-loaded PAA20PPA20 micelles and ATPR solution in CrmEL (with ATPR concentration of 1 mg/mL) were diluted with the cell culturing medium to the concentrations ranging from 4.6 to 4.6×10^{-4} μg/mL. The blank PAA20PPA20 micelles and CrmEL were diluted correspondingly to the concentrations ranging from 9.2 to 9.2×10^{-4} μg/mL. A suitable amount (100 μL) from the four stock solutions were added to each cell. MTT solution (20 μL of a 5 mg/mL) was added to each well after incubation for 72 h at 37 °C.The cells were incubated for an additional 4 h. The supernatant was discarded and 150 μL of DMSO was added to each well to dissolve the formazan crystals. The optical densities (ODs) were checked at 490 nm using a microplate reader (muliskan mk3, Thermo, USA) after a 10 min shaking. Cell viability (%) was calculated as:

$$\text{Cell viability}\,(\%) = \frac{\text{OD } of \text{ test group}}{\text{OD of control group}} \times 100$$

Acknowledgment: Financial support was provided by China Key-Tech Innovation Project for the R & D of Novel Drugs (No. 2008ZX09310–004 and No. 2011ZX09401–021) and the Funds for Outstanding Young Teacher in Higher Education Institutions, AnHui Province (No. 2011SQRL062).

References

Aliferis T, Iatrou H, Hadjichristidis N (2004) Living polypeptides. Biomacromolecules 5: 1653–1656.

Anderson JM, Gibbons DE, Martin RL, Hiltner A, Woods R (1974) The potential for poly-a-amino acids as biomaterials. J Biomed Mater Res A 8: 197–207.

Barrio DJ, Oriol L, Sánchez C, Serrano JL, Cicco AD, Keller P, Li MH (2010) Self-assembly of linear-dendritic diblock copolymers: from nanofibers to polymersomes. J Am Chem Soc 132: 3762–3769.

Daly WH, Poche D (1988) The preparation of N-carboxyanhydrides of α-amino acids using bis (trichloromethyl) carbonate. Tetrahedron Lett 29: 5859–5862.

Deming TJ (2000) Living polymerization of amino acid-N-carboxyanhydrides. J Polym Sci Pol Chem 38: 3011–3018.

Gong J, Huo MR, Zhou JP, Zhang Y, Peng XL, Yu D, Zhang H, Li J (2009) Synthesis, characterization, drug-loading capacity and safety of novel octyl modified serum albumin micelles. Int J Pharm 376: 161–168.

Gref R, Minamitake Y, Percocchia MT, Trubetskoy V, Torchilin V, Langer R (1994) Biodegradable long-circulating polymeric nanospheres. Science 263: 1600–1603.

Harada A, Kataoka K (1997) Formation of stable and monodispersive polyion complex micelles in aqueous medium from poly(L-lysine) and poly(ethylene glycol)-poly(aspartic acid) block copolymer. J Macromol Sci Pure Appl Chem A 34: 2119–2133.

Holowka EP, Sun VZ, Kamei DT, Deming TJ (2007) Polyarginine segments in block copolypeptides drive both vesicular assembly and intracellular delivery. Nat Mater 6: 52–57.

Huo M, Zhang Y, Zhou J, Zou A, Zu D, Wu Y, Li J, Li H (2010) Synthesis and characterization of low-toxic amphiphilic chitosan derivatives and their application as micelle carrier for antitumor drug. Int J Pharm 394: 162–173.

Kataoka K, Kwon GS, Yokoyama M, Okano T, Sakurai Y (1993) Block copolymer micelles as vehicles for drug delivery. J Control Release 24: 119–132.

Kataoka K, Matsumoto T, Yokoyama M, Okano T, Sakurai Y, Fukushima S, Okamoto K, Kwon GS (2000) Doxorubicin-loaded poly(ethylene glycol)–poly(b-benzyl-L-aspartate) copolymer micelles: their pharmaceutical characteristics and biological significance. J Control Release 64: 143–153.

Katayose S, Kataoka K (1998) Remarkable increase in nuclease resistance of plasmid DNA through supramolecular assembly with poly(ethylene glycol)-poly(L-lysine) block copolymer. J Pharm Sci 87: 160–163.

Kidchob T, Kimura S, Imanishi Y (1998) Amphiphilic poly(Ala)-b-poly(Sar) microspheres loaded with hydrophobic drug. J Control Release 51: 241–248.

Kim MS, Dayananda K, Choi EK, Park HJ, Kim JS, Lee DS (2009) Synthesis and characterization of poly(L-glutamic acid)-block-poly-(L-phenylalanine). Polymer 50: 2252–2257.

Li C, Yang DJ, Kuang LR, Wallace S (1993) Polyamino acid microspheres: Preparation, characterization and distribution after intravenous injection in rats. Int J Pharm 94: 143–152.

Li YQ, Bae YH (2006) Polymer architecture and drug delivery. Pharm Res 23: 1–30.

Liu Y, Li JF, Shao K, Huang R, Ye L, Lou J, Jiang C (2010) A leptin derived 30-amino-acid peptide modified pegylated poly-L-lysine dendrigraft for brain targeted gene delivery. Biomaterials 31: 5246–5257.

Makino K, Arakawa M, Kondo T (1985) Preparation and *in vitro* degradation properties of polypeptide microcapsules. Chem Pharm Bull 33: 1195–1201.

Matsumura Y, Maeda H (1986) A new concept for macromolecular therapeutics in cancer chemotherapy: mechanism of tumoritropic accumulation of proteins and the antitumor agent smancs. Cancer Res 46: 6387–6392.

Park JW, Mok H, Park TG (2010) Physical adsorption of PEG grafted and-blocked poly-L-lysine copolymers on adenovirus surface for enhanced gene transduction. J Control Release 142: 238–244.

Ponta A, Bae Y (2010) PEG-poly(amino acid) Block copolymer micelles for tunable drug release. Pharm Res 27: 2330–2342.

Prompruk K, Govender T, Zhang S, Xiong CD, Stolnik S (2005) Synthesis of a novel PEG-block-Poly(aspartic acid-stat-phenylalanine)copolymer shows potential for formation of a micellar drug carrier. Int J Pharm 297: 242–253.

Romberg B, Flesch FM, Hennink WE, Storm G (2008) Enzyme-induced shedding of a poly(amino acid)-coating triggers contents release from dioleoyl phosphatidylethanolamine liposomes. Int J Pharm 355: 108–113.

Romberg B, Metselaar JM, Baranyi L, Snel CJ, Bünger R, Hennink WE, Szebeni J, Storm G (2007) Poly(amino acid)s: Promising enzymeatically degradable stealth coatings for liposomes. Int J Pharm 331: 186–189.

Ruan JJ, Chen HF, Xu J, Shen J,Shi JB,Wu FR,Wang Y (2009) 4-amino-2-trifluoromethyl-phenyl retinate induced K562 cell differentiation and cell cycle influence. Chin Pharmacol Bull 25: 1238–1243.

Schellenberger V, Wang CW, Geething NC, Spink BJ, Campbell A, To W, Scholle MD, Yin Y, Yao Y, Bogin O, Cleland JL, Silverman J, Stemmer WPC (2009) A recombinant polypeptide extends the *in vivo* half-life of peptides and proteins in a tunable manner. Nat Biotechnol 27: 1186–1192.

Schlapschy M, Theobald I, Mack H, Schottelius M, Wester HJ, Skerra A (2007) Fusion of a recombinant antibody fragment with a homo-amino-acid polymer: effects on biophysical properties and prolonged plasma half-life. Protein Eng Des Sel 20: 273–284.

Shen J, Shi JB, Chen FH, Wang Y, Ruan JJ, Huang Y (2009) Synthesis and anti-tumor activity of all-trans retinoic acid derivatives. Chin Chem Lett 20: 805–807.

Shu SJ, Zhang XG, Teng DY, Wang Z, Li CX (2009) Polyelectrolyte nanoparticles based on water-soluble chitosan-poly(L-aspartic acid)–polyethylene glycol for controlled protein release. Carbohyd Res 344: 1197–1204.

Si YC, Samulski ET (2008) Synthesis of water soluble graphene. Nano Lett 8: 1679–1682.

Sun J, Chen XS, Deng C, Yu HJ, Xie ZG, Jing XB (2007) Direct formation of giant vesicles from synthetic polypeptides. Langmuir 23: 8308–8315.

Uchino H, Matsumura Y, Negishi T, Koizumi F, Hayashi T, Honda T, Nishiyama N, Kataoka K, Naito S, Kakizoe T (2005) Cisplatin-incorporating polymeric micelles (NC-6004) can reduce nephrotoxicity and neurotoxicity of cisplatin in rats. Brit J Cancer 93: 678–687.

Wang CY, Gong YB, Fan NQ, Liu SY, Luo SF, Yu JH, Huang J (2009) Fabrication of polymer-platinum(II) complex nanomicelles from mPEG-g-α, β-poly [(N-amino acidyl)-DL-aspartamide] and cis-dichlorod–iammine platinum (II) and its cytotoxicity. Colloid Surface B 70: 84–90.

Wilhelm M, Zhao CL, Wang YC, Xu RL, Winnik MA, Mura JL, Riess G, Croucher MD (1991) Poly(styrene-ethylene oxide) block copolymer micelle formation in water: a fluorescence probe study. Macromolecules 24: 1033–1040.

Yang Y, Cai J, Zhuang X, Guo ZP, Jing XB, Chen XS (2010) pH-Dependent selfassembly of amphiphilic poly(L-glutamic acid)-block-poly(lactic-co-glycolic acid) copolymers. Polymer 51: 2676–2682.